Limnologica 74 (2019) 28–37

Contents lists available at ScienceDirect

Limnologica

journal homepage: www.elsevier.com/locate/limno

Assessing land use and land cover influence on surface water quality using a parametric weighted distance function

Ana L. Liberoff[a,*], Silvia Flaherty[a], Pablo Hualde[b], Martín I. García Asorey[a], Marilyn L. Fogel[c], Miguel A. Pascual[a]

[a] Instituto Patagónico para el Estudio de los Ecosistemas Continentales (CCT-CENPAT-CONICET), Boulevard Brown 2915, (U9120ACV) Puerto Madryn, Chubut, Argentina
[b] Centro de Ecología Aplicada del Neuquén, Provincial Route Nº61 – Km.3 / CC Nº7, (Q8371) Junín de los Andes, Neuquén, Argentina
[c] Environmental Dynamics and Geo-Ecology Institute, Department of Earth Science, University of California, Riverside, 900 University Ave., Riverside, CA, 92521, United States

ARTICLE INFO

Keywords:
Nutrients
Human impacts
Landscape influence
Distance-decay model
Patagonia

ABSTRACT

Stream water quality is directly influenced by land use and human practices in the surrounding environment. Understanding such effects and the spatial extent of impacts is essential to generate reliable information for ecosystem-based management of water resources. We identified sources of impact on water quality and characterized indicator-specific landscape influence on samples collected during base flow along the Chubut River (43 °S, 69 °W). We modeled Total Nitrogen (TN), Total Phosphorous (TP), Soluble Reactive Phosphorous (SRP) concentrations and $\delta^{15}N$ of particulate organic matter along the river, as a function of effective contribution areas (A_{EC}) of Land Use/Land Cover (LULC). A_{EC}s were calculated by assuming that landscape influence decays exponentially with the Euclidean distance between a given LULC parcel and the sampling point. We calibrated the model to the observations by estimating an indicator-specific decay rate. Agriculture and barren lands were the main sources of phosphate nutrients whereas urban areas were the main source of TN. Radius of landscape influence for SRP (100–180 km) was larger than for TP (10–25 km), reflecting different patterns of mobilization and delivery in the catchment. $\delta^{15}N$ variation was explained by vegetation cover but the influence rapidly decreased (1–4 km) reflecting a mostly autochthonous source of organic matter.

1. Introduction

Spatial and temporal variability of stream water quality is determined by natural processes and landscape characteristics within catchments such as land cover, geology, soil type, atmospheric deposition, climate and topography. These landscape characteristics affect the source, mobilization and delivery of nutrients and other constituents from catchments to streams and rivers (Lintern et al., 2017). Land changes and land management affect these natural processes by providing external sources of nutrients (e.g., municipal and industrial sewage effluents, addition of fertilizers; Drewry et al., 2006), affecting mobilization (e.g., erosion due to livestock presence; Fuls, 1992) and delivery (e.g., increased hydrological connectivity in agricultural catchments; Ocampo et al., 2006). The nutrient enrichment of waters causes acidification and eutrophication resulting in a decline in overall water quality restricting its use for general and drinking purposes and degrading aquatic ecosystems (Allan, 2004; Strayer et al., 2003). In this regard, nitrogen and phosphorus are particularly relevant as both are drivers of aquatic eutrophication (Levine and Schindler, 1989) and are linked to the health of humans and other organisms.

Effective nutrient assessment and management is challenging given that nutrients in rivers may originate from a variety of sources, take numerous pathways, and transform from one chemical species to another. A great effort has been made to model the relationship between stream water quality and landscape configuration in order to distinguish sources of pollution and assess their impact on ecosystem functioning. Simple and most popular methods use lumped variables (e.g., % Land use/Land cover, LULC) for landscape representation within a pre-designated influence area (e.g., subwatershed: Wang, 2001). These methods do not take into account the fact that the influence of the landscape depends not only on the sources of impact but also on their location and distance to the river. A great deal of research has been

* Corresponding author.
E-mail addresses: liberoff@cenpat-conicet.gob.ar (A.L. Liberoff), flaherty@cenpat-conicet.gob.ar (S. Flaherty), pablohualde@yahoo.com.ar (P. Hualde), garciaaz@cenpat-conicet.gob.ar (M.I. García Asorey), marilyn.fogel@ucr.edu (M.L. Fogel), pascual@cenpat-conicet.gob.ar (M.A. Pascual).

https://doi.org/10.1016/j.limno.2018.10.003
Received 30 December 2017; Received in revised form 13 September 2018; Accepted 5 October 2018
Available online 15 November 2018
0075-9511/

conducted to capture the spatial scale of landscape-level drivers developing a variety of spatial statistical models (Blanchet et al., 2008; Ver Hoef et al., 2006). Distance-weighted approaches use a mathematical function to assign weights to LULC values according to the distance to the sampling point. Previous studies that have accounted for variations in landscape configuration using distance weighting measures showed an improvement in models predictions compared to traditional methods (Grabowski et al., 2016; Peterson et al., 2011). Distance-weighted metrics have been calculated based on Euclidean measures (King et al., 2005; Peterson et al., 2011), estimates of flow length (Zhang, 2011) and hydrologically active distances (i.e., the distance that water would hypothetically travel throughout a landscape, Grabowski et al., 2016; Peterson et al., 2011). The decline in influence of surrounding landscape has been represented by a variety of decay functions; both inverse distance and exponential functions assume a smoothly decreasing influence with increasing distance (King et al., 2005; Van Sickle and Burch Johnson, 2008). The exponential model is especially appropriate for weighting land use effects on nutrients that are gradually depleted along flow paths or transmitted from a landscape area to the stream channel (Soranno et al., 1996; Zhang, 2011). Besides, the exponential function can be subjected to an optimization procedure to estimate the characteristic influence distances for given in-stream indicators (Van Sickle and Burch Johnson, 2008).

The Chubut watershed in the homonymous Patagonian province of Argentina is the main source of fresh water for 250,000 people and supports a wide variety of activities, including agriculture, cattle-ranching, hydropower production and urban sprawl. Although there is a growing concern about those human activities and practices that are known to affect water quality and stream condition, there is a lack of integral surveys and analyses of water quality throughout the watershed, an obvious information void for water management and conservation.

In this study we applied an exponential distance weighting function based on Euclidean distance metrics to identify both LULC impacts on water quality and the extent of landscape influence. The novel aspect of this study is a model optimization that allows identifying sources of nutrient variation while also estimating the typical radius of landscape influence for each water quality indicator. With this approach we aimed to a) account for dilution and/or metabolization rates from the source to the river network and in-stream, b) allow for specific behaviors for different water quality parameters and c) estimate the absolute contribution of each nutrient for each source (LULC type). We used soluble reactive phosphorous (SRP), total phosphorous (TP), total nitrogen (TN), and nitrate (NO_3^-) concentrations as measurements of water quality and evaluated the use of nitrogen stable isotopes in particulate organic matter (δ^{15}N-POM), as an indicator of terrestrial and in-stream sources of riverine organic matter (Kendall et al., 2001). This analytical framework was applied on data gathered following a Lagrangian field design (Fig. 1).

2. Materials and methods

2.1. Study site

The Chubut River originates in the western extra Andean region of Patagonia (Rio Negro province) and flows for about 1000 km, first south and then east across the Chubut province and into the Atlantic Ocean (Fig. 1). The average discharge is 46.4 $m^3 s^{-1}$ and the total area of the Chubut basin is 57,400 km^2. Given the basin´s geomorphic and climatic characteristics, in particular the west – east precipitation gradient, it is divided into 3 major sub-basins, upper, middle and lower (Coronato and del Valle, 1988). The main tributaries are located in the upper basin. The central drainage basin crosses the Patagonian tableland (heights ranging from 200 to 600 m a.s.l.) without receiving any significant tributary. At 145 km from the estuary, the Florentino Ameghino dam forms a 71 km^2 reservoir lake, inaugurated in 1963 for energy production, flood control, irrigation, and water provision. The lower basin is characterized by alluvial plains and fluvial terraces, with heights ranging from 20 to 150 m.a.s.l.

In terms of discharge, the Chubut River's hydrograph presents two annual peaks, one in spring due to snowmelt and the other in late fall due to rainfall. Precipitation in the watershed shows a marked gradient over a short distance: mean annual rainfall is 500–600 mm in the headwaters, 150 mm in the middle basin and, 250 mm in the coastal area. Most of the Chubut River is on the Patagonian Steppe, where the low precipitation has resulted in xerophytic, herbaceous-shrub-like steppe vegetation. In several parts of the upper and middle basins, the riparian corridor consists solely of the exotic willow, *Salix fragilis*, but in some lower sections the native willow *S. humboldtiana* is also present. The Chubut River watershed is under the influence of strong and dry westerly winds. In comparison to other regions in the world, wind in Patagonia is a relevant meteorological factor given its high intensity and persistence (15–22 km h^{-1} mean annual speed, 65 and 75% of the daily observations in the year, Paruelo et al., 1998).

2.1.1. Watershed land use and land cover

Forests cover a relatively small portion in the headwaters of the watershed (Fig. 2). There are also some croplands in the upper basin, representing a third of the total agricultural land cover in the watershed. The middle basin is dominated by bare lands, followed by shrubland and grassland with almost no agricultural or urban areas but some rural residential areas are associated to sheep ranching (Fig. 2). Traditionally based on continuous grazing, sheep grazing is the main economic activity in the upper and middle basins and is one of the main drivers of vegetation cover modification (Bertiller and Bisigato, 1998) which has exposed denuded soil to surface runoff and wind erosion (del Valle et al., 1997). In the lower basin, croplands and urban areas become more significant (Fig. 2). This area concentrates 50% of the agricultural activity of the Chubut province, with alfalfa and horticulture as the main crops (C.F.I. (Consejo Federal de Inversiones), 2013). Cattle ranching and feedlots are increasingly common in the lower basin. Agriculture in the lower valley is based almost completely on flood irrigation. Man-made water return channels have not been completed, creating a diffuse water return system throughout the agricultural valley. In the upper section of the lower valley, between the Florentino Ameghino dam and the beginning of the agricultural area, there are important deposits of kaolin clay (Fig. 2), which have been exploited by open-cast mining since 1939 (Domínguez and Cavero, 1999).

2.2. Land use / land cover data

A land use / land cover map was generated by combining data obtained from three sources of information. A base land cover layer was taken from the Latin America and the Caribbean map of the SERENA Project (Blanco et al., 2013) which, for the Chubut basin, includes seven categories at a spatial resolution of 500 m: wetland, temperate shrubland, temperate broadleaf evergreen forest, temperate broadleaf deciduous forest, temperate grassland, salt flat and barren land. Given that the SERENA project map lacks land use information, we analyzed high resolution satellite images within QGis (v.2.6.1, OpenLayers Plugin) and digitized polygons for urban areas, rural residential areas, cropland and clay mining areas. The list of clay mines (active and abandoned) and their location were obtained from the website of the Ministry of the Environment and Sustainable Development of the Chubut province. Polygons from each land use category were rasterized at a spatial resolution of 500 m and then overlapped with the SERENA land cover map. For this study we analyzed eight LULC categories as drivers (i.e. predictors) of water quality in the Chubut river watershed (Fig. 1): temperate shrubland, evergreen and broadleaf deciduous forest (merged together into “temperate forest” category), temperate grasslands, barren land, urban areas, rural residential areas, mining and

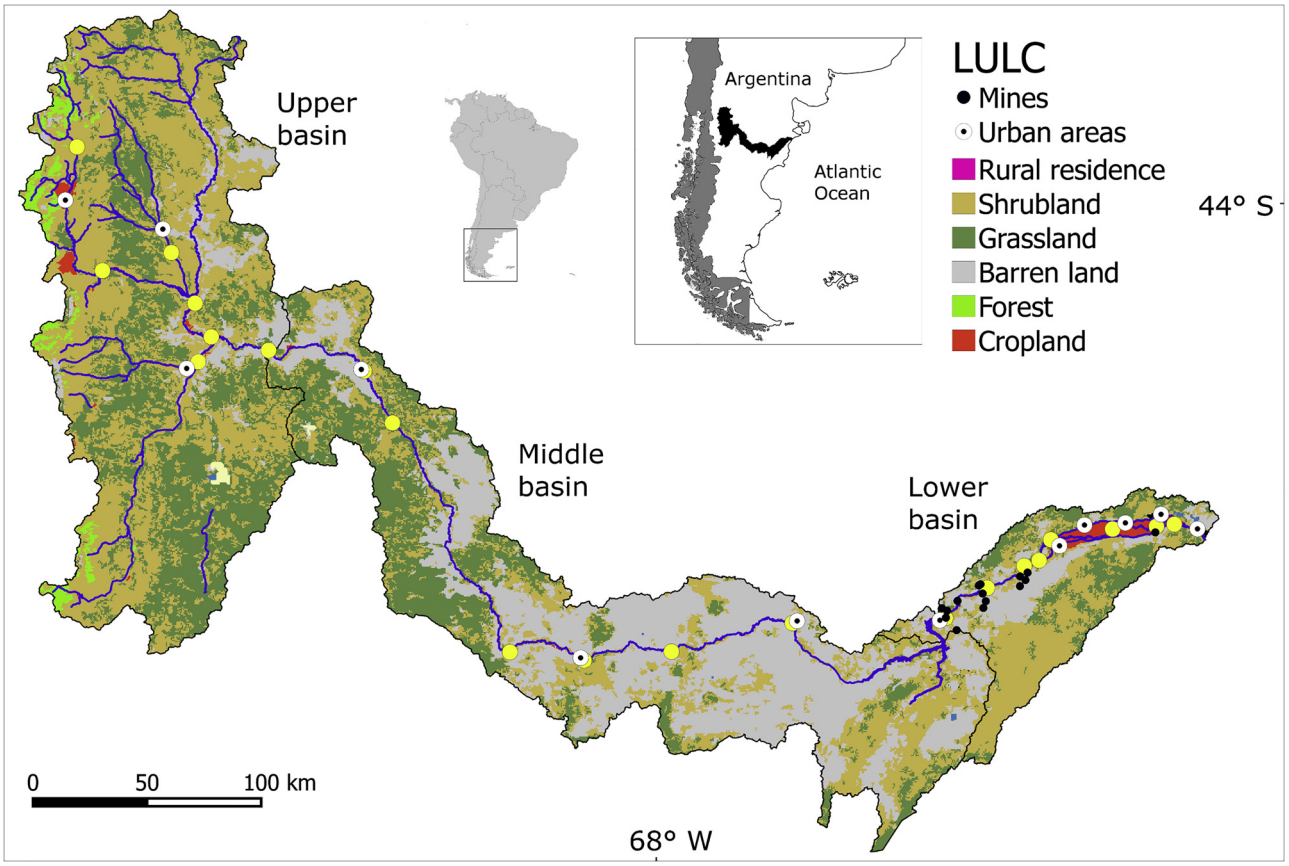

Fig. 1. Location of study site in Patagonia Argentina. Land use / land cover map is shown for the Chubut watershed. Sites sampled for water quality indicators on April 2015 are represented as yellow dots. (For interpretation of the references to colour in this figure legend, the reader is referred to the web version of this article).

cropland. We did not include wetlands and salt flats because they are not accurately mapped at the regional scale of the SERENA classification (analyses not shown).

2.3. Sampling and water quality indicators

A continuous synoptic sampling regime was designed in order to identify hot spots and spatial variation in natural factors and human impact sources. Twenty one sites were sampled along the Chubut River and main tributaries in early fall (8–23 April 2015) covering the total extension of the Chubut River (Fig. 1). We decided to sample in early fall, before the wet season and during baseflow conditions, in order to capture a "base line state". To design the sampling configuration we used the land use/land cover information contained in the LULC map (see previous section). We also explored bankfull channel widths, riparian vegetation cover and slope. Bankfull channel width and riparian vegetation were measured by analyzing high resolution satellite images within QGis (v.2.6.1, OpenLayers Plugin) and slope was calculated using the SRTM 30 m Digital Elevation Model (U.S. Geological Survey, 2014). In order to select the location of sampling sites we explored the distribution of land uses, riparian vegetation, bankfull width and slope measurements plotting them against river distance from the mouth to detect homogeneous river segments and/or discontinuities. Sample sites were then chosen to represent the identified river segments in the catchment.

Water samples were gathered to carry on SRP, TP, TN, NO_3^- and $\delta^{15}N$ – POM analyses. For SRP, NO_3- and $\delta^{15}N$-POM determinations, 3 L of water were filtered through a pre-combusted GF/F filter (0.7 µm). Aliquots of the filtered water were stored frozen for SRP and NO_3^- analysis until laboratory determination was carried out. Filters were stored folded in aluminum foil, frozen and then freeze dried. For TP and TN analyzes, unfiltered water was fixed with sulfuric acid (1 ml of concentrated acid in 500 ml of sample) and stored frozen until their determination. Four TP and TN samples and three POM samples from the middle basin were accidentally spoiled during sampling.

In the laboratory, SRP, TN and TP samples were analyzed following the methodology described in APHA (2004). NO_3^- samples were analyzed at UC Davis Analytical Lab using the flow injection analyzer method with a detection limit of 0.05 mg/L NO_3- - N. For stable isotope analysis, the top layer of a quarter of the filter was removed and placed in a tin boat, followed by combustion in an elemental analyzer (Costech ECS 4010) coupled to a Thermo Fisher Delta V Plus isotope ratio mass spectrometer at the Stable Isotope Laboratory facility within the University of California, Merced. Stable isotope ratios are expressed as $\delta^{15}N$ values, measures of ‰ (ppt) difference between the nitrogen isotope ratios of a sample relative to standard N_2 of the atmosphere (Mariotti, 1983). The working standard were acetanilide ($\delta^{15}N$ = -0.75‰), Glycine ($\delta^{15}N$ = 11.25‰) and Peach ($\delta^{15}N$ = 1.98‰). Repeated analyses of the standards during these analyses showed a standard deviation of ± 0.47, ± 0.06 and ± 0.76 respectively.

2.4. Conceptual model

In order to model the effect of land use and land cover on water quality and to assess the extent of the landscape influence we made three general assumptions/simplifications, which led us to the model represented in Fig. 3:

1) Water quality at a given sampling point in the river is affected by the watershed area upstream from that point and the influence of a given site within the upstream area is inversely related to the distance to the point of interest.

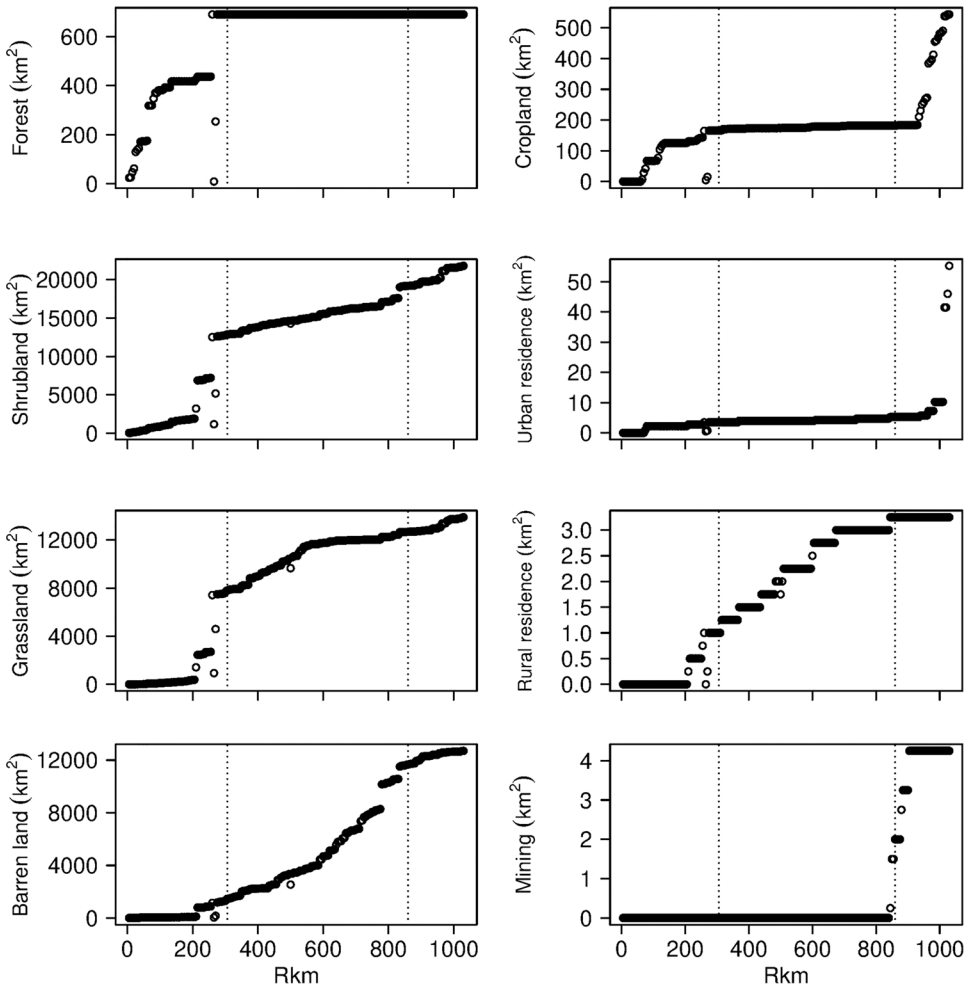

Fig. 2. Accumulated areas of land use and land cover delineated every 5 km from headwater (Rkm = 0) to the mouth (Rkm = 1025). Dashed lines show the limits between the upper-middle and middle-lower basins.

2) The landscape effect decays exponentially with distance (linear in logarithmic scale). The effect of each upstream pixel on any in-river sampling point depends on the Euclidean distance between them.
3) The intercept of the decay function depends on the LULC-indicator combination, whereas the rate of decay with distance depends exclusively on the indicator. In other words, the LULC class of a given pixel determines the initial concentration of each specific nutrient supplied to locations downstream, whereas the fate of a given nutrient as it moves downstream (rate of dilution or metabolization) depends only on the indicator and not on its source.

2.5. Landscape influence: distance weighted effect

Given the conceptual model described above (Fig. 3), we modeled the effect of pixels of different LULC classes upstream of the sampling point by a weighing function. For a given indicator, the effect of pixel i on a given in-river sampling point *j* is controlled by the weight:

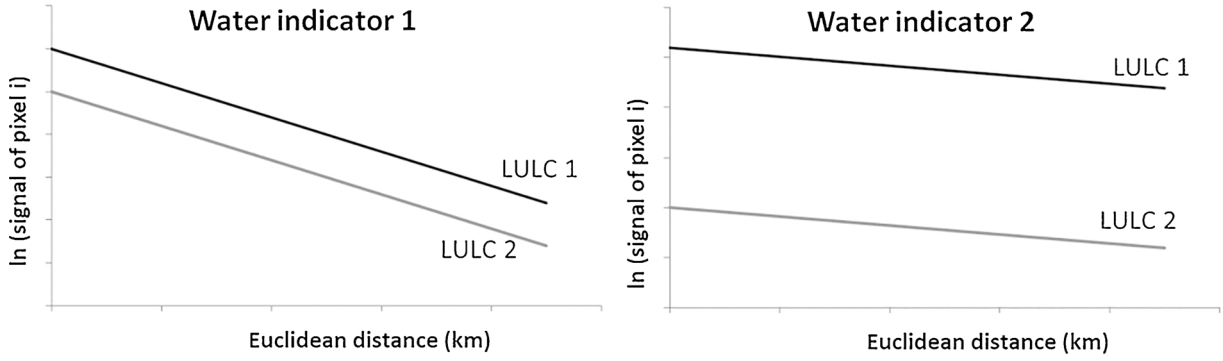

Fig. 3. Schematic representation of the general model applied to evaluate the effect of a pixel i on water quality at any point in the stream. The effect of a given pixel i on the water quality measured in a sampling point depends on 1) the LULC class which regulates the intercept of the decay function for a specific water quality indicator (initial nutrient concentration), 2) the nutrient, which defines the intercept in combination to the LULC class and the slope of the decay rate, and 3) the Euclidean distance between the pixel i and the sampling point.

$$W_i = 0.5^{(dij/D1/2)} \quad (1)$$

Eq. (1) is the exponential curve reparametrized as a function of the half-life. The weight (W_i) decays exponentially as a function of the Euclidean distance between the pixel i and the sampling point *j* (d_{ij}) and a decay parameter specific to each indicator ($D_{1/2}$ or Half Distance). $D_{1/2}$ represents the distance in km at which the concentration of the indicator decays to 50% of the initial concentration (intercept of the decay function in Fig. 3) and expresses the extent or radius of landscape influence in kilometers.

For a given indicator, an ***effective contribution area (A_{ec})*** of LULC class k to a given in-river sampling point is calculated as the sum of all n upstream pixels of class k, weighed by their distance to the point with Eq. (1):

$$A_{ec(k)} = a \sum_{i=1}^{n} W_{i(k)} \quad \text{this study} \quad (2)$$

The parameter ***a*** in Eq. (2) is the unit pixel area (in our case 0.25 km^2), so the effective contribution area is measured in km^2. In summary, the effective contribution area by a LULC class to a given sampling point and for a given indicator will depend on the area and configuration of upstream pixels of that LULC class and by the indicator-specific decay rate. A schematic representation of the application of the weighing procedure in Eqs. (1) and (2) is provided in Fig. 4.

For each sampling point a polygon representing the drainage area (i.e. watershed) was delineated using the SRTM 30 m Digital Elevation Model (U.S. Geological Survey, 2014) and the Batch Watershed Delineation (BWD) tool available in the ArcHydro toolset (in Arc Map 10.1). The LULC map (raster) was converted into a point file and attributes (UTM coordinates and class value) were assigned to each point. For each sampling point we extracted the LULC points falling within the corresponding watershed and exported the attribute tables as text files (one text file for each watershed/sampling point). Finally, we calculated Euclidean distances for each LULC point to the sampling points. These files were used as the inputs to calculate: 1) the W factor for each pixel relative to each sampling point (Eq. (2)) and 2) the effective contribution areas of each LULC class within each watershed and sampling point (Eq. (1)).

Weighted percentages of LULC have been used to model the effects of LULC on water quality (e.g., Grabowski et al., 2016; Peterson et al., 2011). However, using the percentage of a LULC type as explanatory variable does not fully represent the declining effect of individual LULC types because it conceals the actual area of given LULC classes affecting a sampling point. For instance, a small percentage of a given LULC class can result from either a small area of that class (small potential for influence) within a small watershed or a large area (large potential for influence) within a much larger watershed. In other words, when using percentages, explanatory variables are not independent among themselves; i.e. the portrayed response to individual variables is affected by the value that the other ones take. Therefore, in this study and for the purpose of identifying a typical radius of landscape influence for each water quality indicator, we used weighted areas (effective contribution areas) of LULC instead of weighted percentages.

2.6. Data analysis

To model the variation in water quality as a function of LULC, we fitted multiple regression models with the concentration of TP, TN, SRP and δ^{15}N-POM measured at each sampling point as separate response variables and effective contribution areas of the 8 LULC classes considered upstream from each sampling point (Eqs. (1) and (2)) as the independent variables. Separate models were fitted for each of the 4 water quality indicators. Each of the four models has 9 free parameters to be estimated: one Half Distance ($D_{1/2}$) characteristic of the indicator (i.e., the decay rate of the nutrient, Fig. 3) and eight LULC-dependent constants that control the initial concentration of the indicator (i.e., intercept of the decay function in Fig. 3) provided by each of the eight LULC classes.

Most of the sample sites were located on the same stream line, hydrologically connected, and might therefore, be spatially correlated. To accommodate this structure in the data, we fitted the models using a generalized least squares (GLS) technique which allows for dependence between observations (Pinheiro and Bates, 2000). Within the GLS

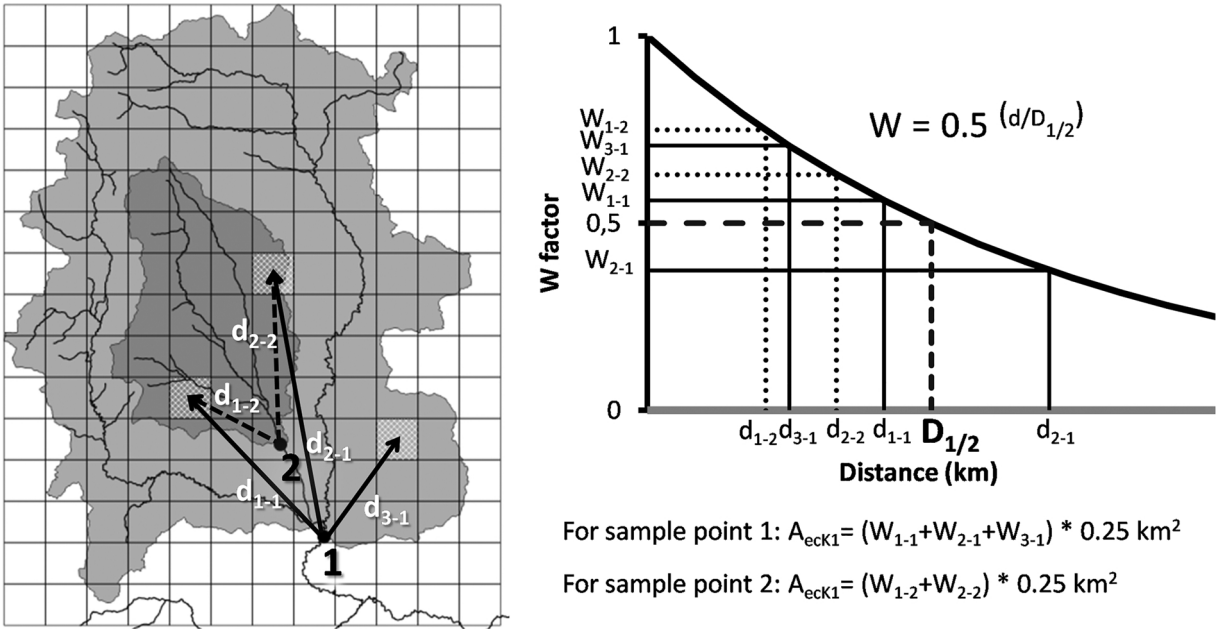

Fig. 4. Schematic calculation of a specific LULC effective contribution area for a given water quality indicator. The figure shows two sampling points and their associated drainage areas (watersheds). A grid representing the LULC map is shown and three shaded pixels represent a given LULC class. Since sampling points are located on the same streamline, the associated watersheds overlap and watershed 1 contains watershed 2. The W factor decays exponentially with the linear distance to the sampling point and the shape of the exponential function is determined by the decay parameter $D_{1/2}$. The effective contribution area is calculated by adding up the relative contribution (W factor) of each pixel classified as K1 falling into the corresponding watershed (three pixels for watershed 1 and two pixels for watershed 2) multiplied by the pixel´s area. The exponential function (the decay rate) is specific to each nutrient type and homogenous for different LULC classes.

framework, we added an exponential spatial residual structure indexing each observation by a two dimensional spatial location vector (x and y coordinates). Models were fitted in R software (R Development Core Team, 2016) using the "gls" function within the "nlme" package (Pinheiro et al., 2016).

For each water quality indicator we performed a model selection routine according to the Akaike Information Criteria with correction for small sample size (AIC_c). AIC defines that the model with the smallest AIC value gives the most parsimonious description of the data. In general, models with Δ AIC (AIC differences) of > 10 have essentially no support and can be omitted from further consideration; models with Δ AIC < 2 have substantial support, while models with 4 < Δ AIC < 7 have considerably less support (Burnham and Anderson, 2002).

The aim of the model selection routine, as applied to each of the water quality indicators, was two-fold: 1) identifying the sources of impact (LULC classes) and 2) estimating the spatial extent of landscape influence through the value of $D_{1/2}$ in Eq. (2) that best explains the variation in water quality along the watershed.

In order to analyze the landscape influence for each water quality indicator we selected 25 values for the parameter $D_{1/2}$ (see Eqs. (1) and (2)) ranging from 0.5 to 180 km to evaluate model goodness of fit and search for the maximization in the correlation between water quality and LULC classes. For each water quality indicator, we fitted all possible models, using Maximum Likelihood estimations, with the full model as a starting point. The selection routine allowed identifying a set of models (the ones with $\Delta AIC_c < 2$) with the combination of LULC classes and values of $D_{1/2}$ (representing the scale of landscape influence in km) that best explained variation in water quality along the watershed. Final model estimations were done through Restricted Maximum Likelihood (REML) estimations. Model ranking was done in R software (R Development Core Team, 2016) using the "dredge" function within the "MuMIn" package (Barton, 2016).

3. Results

3.1. Spatial variation of water quality indicators

Considerably different spatial patterns were found for the different water quality indicators along the river. SRP and TP concentrations exhibited a marked increase in the downstream direction (Fig. 5a and b). TN on the other hand, increased gradually within the upper basin (91.9–285.1 μg/L), but this trend did not persist along the length of the Chubut River, with the exception of the last sampling point which showed an abrupt increase in TN (481.1 μg/L) (Fig. 5c); this sampling point was located just downstream of Trelew, the largest city in the watershed. All NO_3^- samples were below the detection limit (< 0.05 mg/L). The nitrogen isotopic signature ($\delta^{15}N$) of POM was more positive (4‰) in headwaters decreasing gradually as the river flowed through the upper and middle basin before increasing again in the lower basin reaching similar values of $\delta^{15}N$ as in the upper sections of the river (Fig. 5d).

3.2. Water quality modeling

SRP variation was largely explained and positively related to cropland and barren land in upstream areas (Models 1–6, Table 1; Figs. 5a and 6). $D_{1/2}$ value ranged from 100 to 180 km indicating a large spatial landscape influence for this indicator. TP variation was better explained by cropland, forest and barren land (Figs. 5b and 7 ; Models 7–10, Table 1) for shorter radius of influence (10–19 km). For longer distances (22–25 km) only cropland and barren land were important (Models 11 and 12, Table 1).

For TN, the model selection did not yield a consistent set of models (Models 13–36, Table 1). All values of $D_{1/2}$ yielded similar models in terms of AIC and explanatory variables changed with the extent of landscape influence. However, urban area was the most important variable and was present in every model. For shorter distances, mining, barren land and forested areas were also important (Models 13–18, Table 1, 1–16 km,). As the radius of influence increased to intermediate distances (25–31 km, Models 21–23, Table 1) rural areas became significant. For $\delta^{15}N$-POM model selection yielded two models that better explained N signature of POM along the watershed (Models 37 and 38, Table 1, Figs. 5d and 8). The $\delta^{15}N$ signature was more depleted as barren lands, grassland, and forested areas increased. The extent of landscape influence for this indicator was 1–4 km.

4. Discussion

In this study we used a spatially explicit framework based on a parametric distance weighted metric to explain the relationship between water quality and LULC in the Chubut River and its main tributaries. The methodology we applied allowed us to identify not only the human impacts and the vegetation cover effects on water quality but also the spatial extent of landscape influence for each water quality indicator.

In order to model the distance-related landscape influence we applied an exponential decay rate based on Euclidean distances. The exponential function is the simplest approach to represent a decaying effect with a constant rate and it has proven to perform well when modeling progressive depletion of nutrients caused by land or in-stream processes (Peterson et al., 2011; Smith et al., 1997; Van Sickle and Burch Johnson, 2008; Zhang, 2011). Euclidean distances have also shown to capture the same amount of water quality variation than total flow-path distances (King et al., 2005). However, this metric might be underestimating the extent of landscape influence given that overland and in-stream flows represent longer distances than linear measures. In this regard, the extents of landscape influence detected in this study are the "minimum". Nevertheless, they provide a valid metric for the identification of the specific scales of landscape influence for each water quality indicator (e.g., tens of kilometers for TP vs. hundreds of kilometers for SRP). Calculation of flow-path distances would allow for a better discerning of LULC overland flow **to the stream** from **in-stream** processes (Van Sickle and Burch Johnson, 2008). Isolating both effects would lead to a more realistic modeling of nutrient transportation because different processes might be taking place in each of the transport phases. In our system, irrigation channels in the agricultural valley, that divert the original flow of water in the stream network, make it difficult to calculate actual flow-path distances. Further research is being carried out to incorporate the irrigation channels into the stream network by modifying the DEM using ArcHydro tools (ArcMap 10.1).

Cropland and barren land explained the majority of SRP and TP variation along the watershed, reflecting the pollutant load from agricultural lands and the export of sediment-bound nutrients from barren lands. In the lower valley, irrigation practices and artificial channel networks facilitate the delivery of nutrients loaded from croplands to the stream. On one hand, irrigation practices artificially recharge groundwater, increasing water table levels (Hernández et al., 1983). Higher interaction between ground and surface water and increased subsurface flow affect delivery rates of dissolved nutrients leading to increased concentrations in the stream (Ocampo et al., 2006). In addition, man-made drainage systems might have also affected the delivery of both particulate and dissolved nutrients by increasing surface flow and hydrological connectivity between croplands and the stream.

Sheep grazing is one of the major causes of desertification in semiarid Patagonia (Benites et al., 1993) and is a serious environmental concern. As plant cover decreases, soil degradation progresses (Verón and Paruelo, 2010). Once soil is denuded, erosion caused by water and wind increases markedly thereby diminishing the superficial soil layer and causing increased evaporation, runoff, soil erosion, and nutrient loss (Fuls, 1992). It is estimated that wind erosion affects nearly 50% of

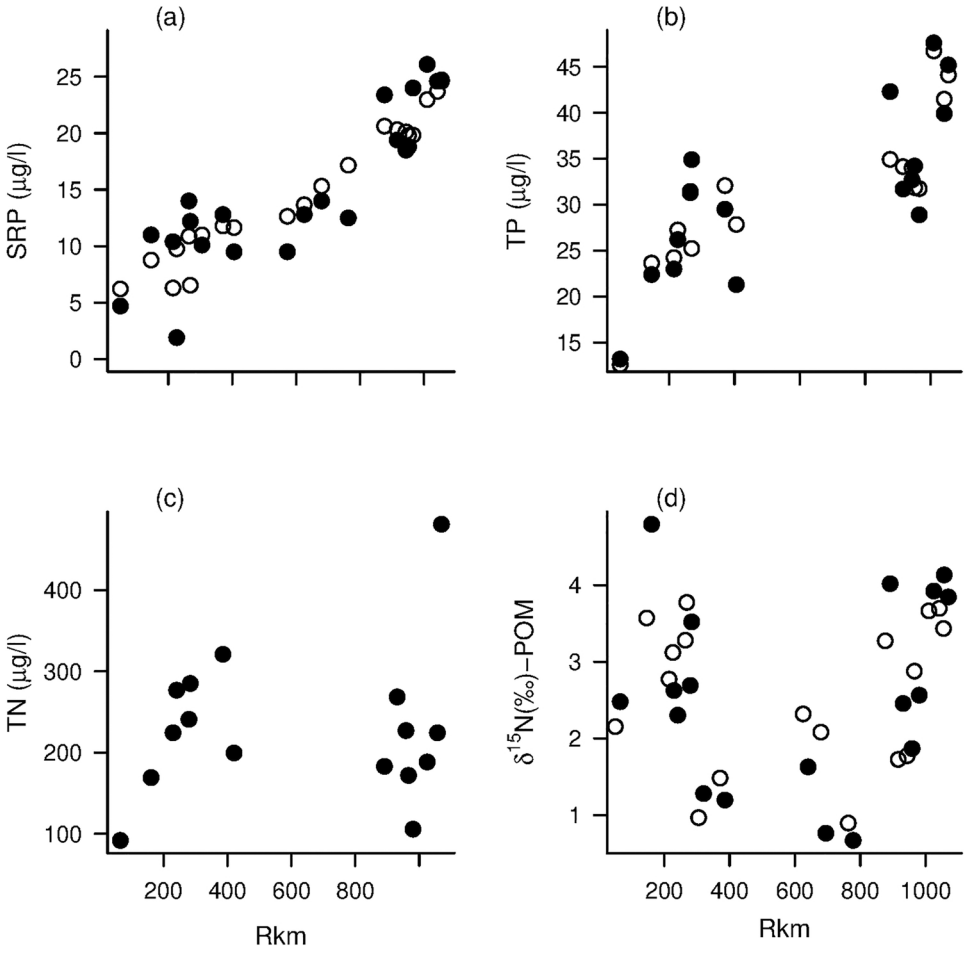

Fig. 5. Observed (black dots) and estimated (empty dots) concentrations of (a) soluble reactive phosphorous (b) total phosphorous (c) total nitrogen and (d) $\delta^{15}N$ of particulate organic matter along the Chubut River estimated by generalized least squares using restricted maximum likelihood. SRP = 6.13 + 2.26 cropland + 0.20 barren land, areas were calculated with a $D_{1/2}$ value of 180 km (Model 6, Table 1). TP = 23.61 + 19.04 cropland – 18.21 forest + 3.42 barren land, areas were calculated with a $D_{1/2}$ value of 13 km (Model 8, Table 1). $\delta^{15}N$ – POM = 4.53–18.49 forest –4.56 grassland – 4.12 barren land, areas were calculated with a $D_{1/2}$ value of 4 km (Model 38, Table 1). Observed values for panel (d) are slightly moved in the x-axis to allow visualization of overlapping points.

the Chubut province area (FAO, 1993). Therefore, it is likely that aerial transport has a large effect on the total nutrient exported to the stream and that our models is capturing both water and wind erosion processes. Sediment export to the stream during rain events is an acknowledged problem by the local community, where high sediment concentrations disrupt the normal operation of water treatment plants compromising drinking water supply in the lower valley (Kaless et al., 2008). However, the consequences of desertification in terms of nutrient loss or exportation to the stream had not been previously addressed. Our study identified that barren lands are an important source of phosphate nutrients which, coupled with agricultural loads, affect water quality in the lower valley where the effects magnify and accumulate (see Results section).

Landscape influence on SRP concentrations has a reach of over 180 km, representing a large scale of impact and also reflecting that SRP accumulates along the stream pathway. The accumulation of SRP in river water could be due to 1) the homogeneous flux of dissolved nutrients from barren lands along the middle and lower basins and/or 2) the low utilization of inorganic P by the stream biota. Miserendino (2007) showed a decrease in macroinvertebrate diversity and species richness in the Chubut middle basin and attributed it to low resources and high levels of suspended particles production. Her findings support the hypothesis of low efficiency in the utilization of inorganic P exported from barren lands. While SRP was affected by areas further upstream, TP was related to more local landscape influences (10–25 km). A radius of influence between 10 and 25 km for the lowermost sites provides evidence that TP is mainly exported from barren lands within the lower basin itself. In the upper basin, forest cover decreases TP concentration in the stream. As vegetation cover protects soil from runoff and wind erosion, it decreases particulate nutrients mobilization from the catchment to the stream (Lintern et al., 2017). According to the analysis presented herein, effects of forested lands on water quality are more intense within a radius of 20 km. Given that TP data for 4 sites in the middle basin are missing, the interpretation of the radius of influence for TP is constrained to the effects of LULC on water quality in the upper and lower basins.

Nitrate concentrations were below the detection limit. In ultra-oligotrophic systems, with TN concentrations lower than 1 mg N/l, inorganic N is taken up rapidly to sustain primary productivity (Durand et al., 2011). This might be the case for the lower Chubut River in the fall (end of crop and irrigation season), when the system might be N limited. TN was highly affected by urban areas. Given that NO_3^- concentrations were extremely low, TN was mostly represented by N in either the organic phase or bound to sedimentary particles. Storm water runoff through impervious surfaces and industrial effluents in the lower valley could explain the abrupt increase in organic N in the lowermost sampling point. The inconsistency in TN models might be reflecting that different LULC classes produce different patterns of nutrient transport. For example, Zhang (2011) found that the decay rate in nitrogen transport from urban areas was lower than for other LULC classes. The authors associate this to the higher heterogeneity in land cover composition of urban areas in contrast to vegetated lands. They state that urban area classes are more prone to mask a variety of LULC types with different hydrological conditions of nitrogen transportation (e.g., green areas, impervious surfaces) than agricultural or forested areas. In this study we assumed the same decay rate for different LULC classes but future studies with higher resolution of field data and LULC maps should test different values of $D_{1/2}$ for different LULC classes. To address these more complex scenarios, sampling with higher spatial resolution is already being carried out in the lower basin.

Table 1
Final model selection explaining water quality variation in the Chubut watershed as a function of Land Use / Land Cover (CL: cropland, BL: barren land, F: forest, M: mining, RR: rural residential areas, GL: grassland). The table shows the best set of models (Δ AIC < 2) for each water quality variable. Models that have the same explanatory variables (model structure) are shown in the same row; values of the $D_{1/2}$ parameter, degrees of freedom, log Likelihood values and Δ AIC for each model are shown within each row in order of appearance.

Water quality variable	Model number	Model structure	$D_{1/2}$ (km)	df	logLik	ΔAICc
Soluble reactive phosphorous	1–6	CL + BL	100,110,120,140,160,180	18	−54.78, −54.58, −54.42, −54.17, −53.98, −53.84	1.88, 1.48, 1.15, 0.65, 0.28, 0.00
Total phosphorous	7–10	CL - F + BL	10,13,16,19	12	−44.16, −43.93, −44.04, −44.34	0.46, 0.00, 0.23, 0.82
	11,12	CL + BL	22,25	13	−42.29, −47.49	1.39, 1.78
Total nitrogen	13	M - BL + UA	1	12	−81.06	0.00
	14	BL + UA	4	13	−83.76	0.07
	15–18	−F + UA	7, 10, 13, 16	13	−84.02, −84.08, −84.28, −84.56	0.60, 0.72, 1.12, 1.67
	19, 20	UA	19, 22	14	−86.82, −86.82	1.82, 1.83
	21–23	RR + UA	25, 28, 31	13	−84.62, −84.61, −84.63	1.78, 1.77, 1.81
	24–36	UA	34, 37, 40, 50, 60, 70, 80, 90, 100, 120, 140, 160, 180	14	−86.81, −86.81, −86.81, −86.79, −86.78, −86.77, −86.76, −86.76, −86.75, −86.75, −86.77, −86.78	1.82, 1.81, 1.80, 1.78, 1.75, 1.73, 1.72, 1.70, 1.70, 1.70, 1.70, 1.71, 1.72, 1.74
δ^{15}N - Particulate organic matter	37, 38	- F - GL - BL	1, 4	14	−14.46, −15.07	0.00, 1.14

Stable isotopes in the POM fraction are used to trace relative contributions of allochthonous (terrestrial) organic matter and autochthonous materials derived from plankton and algae, aquatic macrophytes, and fragments and fecal matter from invertebrates and fish in the river (Kendall et al., 2001). Other sources of allochthonous dissolved organic matter such as water from waste water treatment plants, sewage overflows in urban areas or confined animal feeding operations and agricultural runoff in farming areas could influence the δ^{15}N of the POM produced in the river (Finlay and Kendall, 1994). While an increase in the δ^{15}N of POM was observed in the lower basin, the overall δ^{15}N variation was mainly explained by vegetation cover and the area of barren land. Interestingly, while variation in TN was related to human settlements (see above), δ^{15}N-POM was not. The local landscape influence for the δ^{15}N-POM indicator (1–4 km) suggests that landscape influence rapidly disappears, probably due to the fact that the δ^{15}N of POM is determined by autochthonous sources. Future research in this river system should evaluate stable isotope indicators at a smaller scale redefining LULC maps to include specific human related categories (e.g., feedlots, crop type, point sources) and increasing spatial resolution.

To summarize, we identified that in-stream SRP and TP concentrations in the middle and lower basins are affected by the same human related activities (agriculture and desertification) and in the upper basin forest cover affect particulate phosphorous concentrations. The differences in landscape influence reflect differences in dissolved and particulate nutrients mobilization, metabolization and delivery processes in the catchment. The source of organic matter in the Chubut River (during baseflow and in the end of the crop season), as indicated by N stable isotopes signatures in POM and its short landscape influence, is mostly autochthonous but in the lower reaches urban areas contribute a large amount of allochthonous organic matter.

In order to improve our understanding of the sources of impact and temporal variation of nutrient transport, it is necessary to increase the amount and quality of the data used as inputs for the models. As a first attempt to understand the relationship between landscape and surface water quality in the Chubut River we used a regional LULC map which lacks resolution for some important local landscape features that affect nutrient retention and exportation such as wetlands. Our map also lacked important human activities such as feedlot operations and location of point sources. This is in our agenda and we are currently working on generating a higher resolution local LULC map for future analyses. Furthermore, seasonality should also be considered when modeling nutrient contribution from the landscape to the stream. Given that we used data from only one season we did not take into account the effect of precipitation and stream events which mainly affect the mobilization and delivery of sediments and particulate nutrients. In this regard, this study reflects the relationship between landscape and water quality during baseflow and lays the foundation for future sampling strategies. As an example, we have learned that if we are pursuing to use stable isotopes in POM as indicators of organic matter sources sampling should be denser in order to capture the spatial variation (1–4 km) detected in this study.

The analytical framework presented here could be useful to delineate future scenarios of land use and evaluate the water quality response. For example, we could evaluate what would be the response of water quality if we restored vegetation and we could also identify sensitive areas to be revegetated (i.e., areas of barren land that minimize nutrient concentrations in the stream when they are replaced by shrubland). In this study we applied a spatial autocorrelation structure by fitting GLS. For more dendritic watersheds, other statistical tools such as Linear Mixed Effects Models (LME) could also be useful to allow for within-group dependence (i.e., samples sites within tributaries) at the same time that autocorrelation structures are included.

Finally, we highlight some specific methodological characteristics of the analytical framework applied: (1) Unlike other conceptually related studies, we used areas of LULC around a sampling point as predictors,

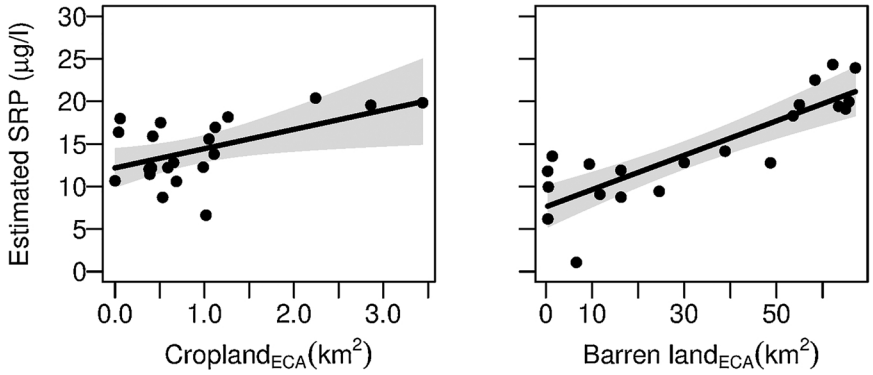

Fig. 6. Partial regression plots of Model 6 (Table 1) showing the partial correlation of cropland and barren land effective contribution areas (ECA) to SRP concentration after removing the linear effects of the other independent variables in the model. Shaded areas represent the 5 and 95% confidence intervals.

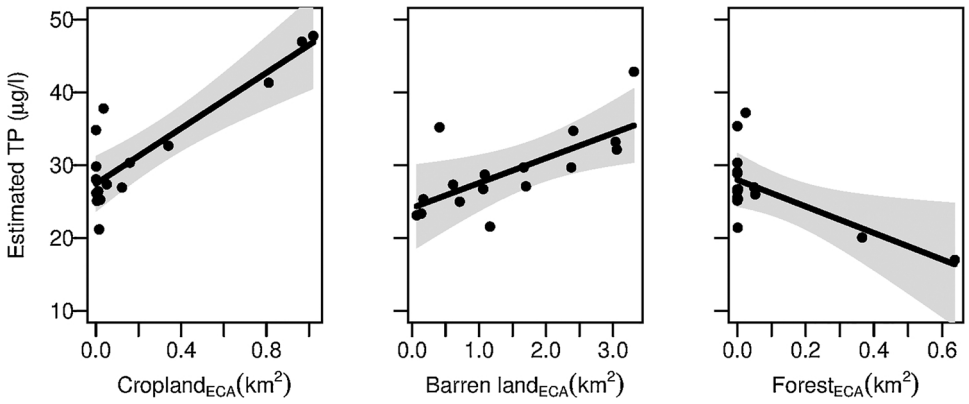

Fig. 7. Partial regression plots of Model 8 (Table 1) showing the partial correlation of cropland, barren land and forest effective contribution areas (ECA) to TP concentration after removing the linear effects of the other independent variables in the model. Shaded areas represent the 5 and 95% confidence intervals.

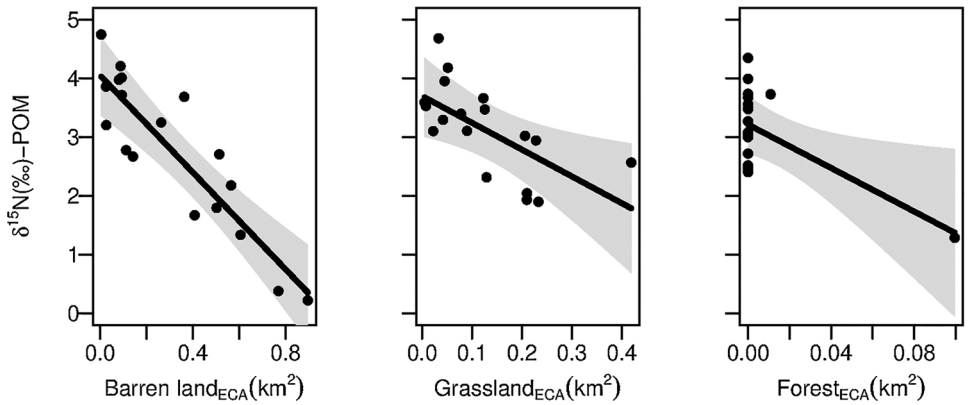

Fig. 8. Partial regression plots of Model 38 (Table 1) showing the partial correlation of barren land, grassland and forest effective contribution areas (ECA) to N signatures of POM after removing the linear effects of the other independent variables in the model. Shaded areas represent the 5 and 95% confidence intervals.

avoiding the issue of collinearity among LULC classes due to lack of independence when class percentages are used (King et al., 2005). (2) A watershed was defined for each sampling point, treated as outlets, and the weighted areas of each LULC category were only calculated based on the cells upstream of each sampling point. This method prevented the inclusion of downstream areas when measuring Euclidean distances centered in a sampling point. (3) A parsimonious approach was chosen by fitting exponential weighting functions on Euclidean distances within watershed boundaries; this simple method might be desirable when there is a constraint in sampling points. (4) We fitted all possible models, evaluating all LULC classes, and compared them through a model selection routine. Multiple regressions allowed us to factor out the effect of one LULC variable and explore the independent regressions among the remaining LULC variables and the water quality residuals (see partial regression plots, Figs. 6–8). Typically, researchers calculate many correlations between several stream indicators and LULC variables (see references in Van Sickle and Burch Johnson, 2008) but simple correlations may lead to incorrect interpretations of the magnitude and the direction of an effect (King et al., 2005). (5) We subjected the $D_{1/2}$ parameter (shape of the exponential curve or rate of decay) to a model optimization procedure which allowed us for the identification of the scale of landscape influence on different water quality indicators; information highly relevant for delineating land management plans.

Acknowledgments

Funding for this research was provided by the International Atomic Energy Agency to A. Liberoff, The Nature Conservancy to M. Pascual, a postdoctoral grant to A. Liberoff from the Consejo Nacional de Investigaciones Científicas y Tecnológicas (CONICET), and the University of California Merced to M. Fogel, and was conducted under the projects “Red para la conservación de los ecosistemas fluviales de la Patagonia” (CONICET) and PUE-IPEEC-CONICET Nº 22920160100044. The authors wish to thank the Dirección de Pesca Continental de la Provincia del Chubut, especially to Walter Frizzera, Jorge Hube, Victoriano Barrera, Walter Curiñanco, Renzo Mendez and Pedro Olivera, and to Juan Pablo Barriga, BereniceTrovant, Celia Beloso and Carolina Giese for sample collection and processing, and David Araiza, UC Merced for isotope analyses. The authors also wish to acknowledge anonymous reviewers for very their contributions which certainly led to an overall improvement of the paper.

References

Allan, J.D., 2004. Landscapes and riverscapes: the influence of land use on stream ecosystems. Annu. Rev. Ecol. Evol. Syst. 35, 257–284.

APHA, 2004. Standard Methods for the Examination of Water and Wastewater, 19th ed. American Public Health Association, Washington, DC.

Barton, K., 2016. MuMIn: Multi-Model Inference. R Package Version 1.9.5.

Benites, J., Saintraint, D., Morimoto, K., 1993. Degradación de suelos y producción agrícola (informe de paises), Erosion de suelos en America Latina. Food and Agriculture Organization of the United Nations. Regional Office for Latin America and the Caribbean, Santiago, Chile. http://www.fao.org/docrep/t2351s/T2351S00.htm.

Bertiller, M.B., Bisigato, A.J., 1998. Vegetation dynamics under grazing disturbance. The state and transition model for the Patagonian steppes. Ecol. Austral 8, 191–199.

Blanco, P.D., Colditz, R.R., López Saldaña, G., Hardtke, L.A., Llamas, R.M., Mari, N.A., Fischer, A., Caride, C., Aceñolaza, P.G., del Valle, H.F., Lillo-Saavedra, M., Coronato, F., Opazo, S.A., Morelli, F., Anaya, J.A., Sione, W.F., Zamboni, P., Barrena Arroyo, V., 2013. A land cover map of Latin America and the Caribbean in the framework of the SERENA project. Remote Sens. Environ. 132, 13–31.

Blanchet, F.G., Legendre, P., Borcard, D., 2008. Modelling directional spatial processes in ecological data. Ecol. Model. 215, 325–336.

Burnham, K.P., Anderson, D.R., 2002. Model Selection and Multimodel Inference: A Practical Information-Theoretic Approach. Springer-Verlag, New York.

C.F.I. (Consejo Federal de Inversiones), 2013. Plan director de recursos hídricos del Río Chubut. Gobierno de la Provincia de Chubut. Rawson. pp. 186.

Coronato, F., del Valle, H., 1988. Caracterización hídrica de las cuencas hidrográficas de la provincia del Chubut. CENPAT-CONICET, Puerto Madryn, Chubut p. 288.

del Valle, H.F., Elissalde, D.A., Gagliardini, D.A., Milovich, J., 1997. Distribución y cartografía de la Patagonia Vol. 28 RIA 1:24.

Domínguez, E., Cavero, F., 1999. Los recursos de caolín de Chubut y Santa Cruz. In: Zappettini, E.O. (Ed.), Recursos Minerales de la República Argentina. Instituto de geología y recursos minerales SEGEMAR, Buenos Aires, pp. 1265–1272.

Drewry, J.J., Newham, L.T.H., Greene, R.S.B., Jakeman, A.J., Croke, B.F.W., 2006. A review of nitrogen and phosphorus export to waterways: context for catchment modelling. Mar. Freshw. Res. 57, 757–774.

Durand, P., Breuer, L., Johnes, P.J., Billen, G., Butturini, A., Pinay, G., van Grinsven, H., Garnier, J., Rivett, M., Reay, D.S., Curtis, C., Siemens, J., Maberly, S., Kaste, O., Humborg, C., Loeb, R., de Klein, J., Hejzlar, J., Skoulikidis, N., Kortelainen, P., Lepisto, A., Wright, R., 2011. Nitrogen processes in aquatic ecosystems. In: Sutton, M.A., Howard, C.M., Erisman, J.W., Billen, G., Bleeker, A., Grennfelt, P., van Grinsven, H., Grizzetti, B. (Eds.), The European Nitrogen Assessment. Cambridge University Press, Cambridge, pp. 126–146.

F.A.O. 1993. "Erosion de suelos en America Latina". Taller sobre la Utilización de un Sistema de Información Geográfica (SIG) en la Evaluación de la Erosión Actual de Suelos y la Predicción del Riesgo de Erosión Potencial, Santiago, Chile, 27 de julio al 1° de agosto de 1992. Proyecto GCP/RLA/107/JPN. ISBN 92-854-3001-5 (http://www.fao.org/docrep/t2351s/T2351S00.htm).

Finlay, J.C., Kendall, C., 1994. Stable isotope tracing of temporal and spatial variability in organic matter sources to freshwater ecosystems. In: Michener, R., Lajtha, K. (Eds.), Stable Isotopoes in Ecology and Environmental Science. Blackwell, pp. 283–324.

Fuls, E.R., 1992. Ecosystem modification created by patch-overgrazing in semi-arid grassland. J. Arid Environ. 23, 59–69.

Grabowski, Z.J., Watson, E., Chang, H., 2016. Using spatially explicit indicators to investigate watershed characteristics and stream temperature relationships. Sci. Total Environ. 551–552, 376–386.

Hernández, M.A., Ruiz de Galarreta, V.A., Fidalgo, F., 1983. Diagnosis geohidrológica aplicada en el valle inferior del Río Chubut. Ciencia del Suelo 1, 83–91.

Kaless, G., Matamala, F.M., Montero, B., Greco, W., 2008. Cambios hidrológicos y morfológicos en el Río Chubut aguas abajo de la presa Florentino Ameghino. V Congreso Argentino de Presas y Aprovechamientos Hidroeléctricos, Tucumán, Argentina.

Kendall, C., Silva, S.R., Kelly, V.J., 2001. Carbon and nitrogen isotopic compositions of particulate organic matter in four large river systems across the United States. Hydrol. Process. 15, 1301–1346.

King, R.S., Baker, M.E., Whigham, D.F., Weller, D.E., Jordan, T.E., Kazyak, P.F., Hurd, M.K., 2005. Spatial considerations for linking watershed land cover to ecological indicators in streams. Ecol. Appl. 15, 137–153.

Levine, S.N., Schindler, D.W., 1989. Phosphorus, nitrogen, and carbon dynamics of experimental Lake during recovery from eutrophication. Can. J. Fish. Aquat. Sci. 46, 2–10.

Lintern, A., Webb, J.A., Ryu, D., Liu, S., Bende-Michl, U., Waters, D., Leahy, P., Wilson, P., Western, A.W., 2017. Key factors influencing differences in stream water quality across space. Wiley Interdiscip. Rev. Water 5, e1260.

Mariotti, A., 1983. Atmospheric nitrogen is a reliable standard for natural ^{15}N abundance measurements. Nature 303, 251–252.

Miserendino, M.L., 2007. Macroinvertebrate functional organization and water quality in a large arid river from Patagonia (Argentina). Ann. Limnol. Int. J. Limnol. 43, 133–145.

Ocampo, C.J., Sivapalan, M., Oldham, C., 2006. Hydrological connectivity of upland-riparian zones in agricultural catchments: implications for runoff generation and nitrate transport. J. Hydrol. 331, 643–658.

Paruelo, J.M., Beltran, A., Jobbagy, E., Sala, O.E., Golluscio, R.A., 1998. The climate of Patagonia: general patterns and controls on biotic processes. Ecol. Austral 8, 85–101.

Peterson, E.E., Sheldon, F., Darnell, R., Bunn, S.E., Harch, B.D., 2011. A comparison of spatially explicit landscape representation methods and their relationship to stream condition. Freshw. Biol. 56, 590–610.

Pinheiro, J.C., Bates, D.J., DebRoy, S., Sarkar, D., R Development Core Team, 2016. Linear and Nonlinear Mixed Effects Models. R Package.

Pinheiro, J.C., Bates, D.M., 2000. Mixed Effects Models in S and S-PLUS. Springer-Verlag New York, Inc.

R Development Core Team, 2016. R: A Language and Environment for Statistical Computing, 3.0. R Foundation for Statistical Computing, Vienna, Austria.

Smith, R.A., Schwarz, G.E., Alexander, R.B., 1997. Regional interpretation of water-quality monitoring data. Water Resour. Res. 33, 2781–2798.

Soranno, P.A., Hubler, S.L., Carpenter, S.R., Lathrop, R.C., 1996. Phosphorus loads to surface waters: a simple model to account for spatial pattern of land use. Ecol. Appl. 6, 865–878.

Strayer, D.L., Beighley, R.E., Thompson, L.C., Brooks, S., Nilsson, C., Pinay, G., Naiman, R.J., 2003. Effects of land cover on stream ecosystems: roles of empirical models and scaling issues. Ecosystems 6, 407–423.

U.S. Geological Survey, 2014. Shuttle Radar Topography Mission (SRTM) 1 Arc-Second Global. https://lta.cr.usgs.gov/SRTM1Arc.

Van Sickle, J., Burch Johnson, C., 2008. Parametric distance weighting of landscape influence on streams. Landsc. Ecol. 23, 427–438.

Ver Hoef, J.M., Peterson, E., Theobald, D., 2006. Spatial statistical models that use flow and stream distance. Environ. Ecol. Stat. 13, 449–464.

Verón, S.R., Paruelo, J.M., 2010. Desertification alters the response of vegetation to changes in precipitation. J. Appl. Ecol. 47, 1233–1241.

Wang, X., 2001. Integrating water-quality management and land-use planning in a watershed context. J. Environ. Manage. 61, 25–36.

Zhang, T., 2011. Distance-decay patterns of nutrient loading at watershed scale: regression modeling with a special spatial aggregation strategy. J. Hydrol. 402, 239–249.